East European Journal of Physics. 4. 701-708 (2025)
DOI:10.26565/2312-4334-2025-4-76 ISSN 2312-4334

A STUDY OF THE WEAR RESISTANCE OF TiMoN/NbN NANO-MULTILAYER COATINGS DEPOSITED BY CA-PVD TECHNOLOGY UNDER DIFFERENT WORKING PRESSURES

O.V. Maksakova[1,2], V.M. Beresnev[2], S.V. Lytovchenko[2]*, M. Čaplovičova[3], D.V. Horokh[2], B.O. Mazilin[2], M. Sahul[1]

[1]*Institute of Materials Science, Slovak University of Technology in Bratislava, 25, Jána Bottu Str., 917 24 Trnava, Slovakia*
[2]*V.N. Karazin Kharkiv National University, 4, Svoboby Sq., 61000 Kharkiv, Ukraine*
[3]*Centre for Nanodiagnostics of Materials, Slovak University of Technology in Bratislava, Vazovova 5, 812 43 Bratislava, Slovakia*
**Corresponding Author e-mail: s.lytovchenko@karazin.ua*
Received May 1, 2025; revised August 13, 2024; accepted October 21, 2025

This study investigates the wear behaviour of TiMoN/NbN nano-multilayer coatings deposited by cathodic-arc PVD under two nitrogen working pressures (0.52 and 0.13 Pa). Although both coatings exhibit comparable total thicknesses (~10–11 μm) and a similar number of periods (~270), their structural integrity, interface coherence, and elemental distribution differ significantly with deposition pressure. The coating synthesized at 0.52 Pa develops a highly ordered, dense multilayer architecture, characterized by well-defined interfaces and a reduced microdefect density. Conversely, the coating deposited at 0.13 Pa displays pronounced interfacial waviness, disrupted periodicity, and increased defect concentration. Ball-on-disc tribological tests reveal a stable friction coefficient of 0.42–0.48 for the 0.52 Pa coating, whereas the 0.13 Pa coating shows an elevated and unstable friction response (0.60–0.70) with frequent fluctuations. Microstructural and chemical analyses of wear tracks indicate the formation of a robust, adaptive Ti–Nb–Mo–O tribofilm for the high-pressure coating, incorporating lubricious MoO_3 and mechanically strengthening Nb_2O_5 phases. In contrast, the low-pressure coating produces only a thin, brittle TiO_2-rich film lacking self-replenishing capability. These findings demonstrate that optimized nitrogen pressure is essential for achieving structurally coherent nanolaminates capable of forming functional tribofilms, thereby dramatically improving wear resistance in TiMoN/NbN nano-multilayer systems.
Keywords: *PVD; Nitrides; Multilayer coatings; Microstructure; Composition; Wear*
PACS: 68.55.Jk, 68.65.Ac

INTRODUCTION

In modern mechanical engineering, instrument engineering, aviation, and power engineering, materials capable of withstanding extreme operating conditions – high temperatures, abrasive and corrosive wear, and cyclic loading – are playing an increasingly important role [1]. To protect tools, components, and assemblies, hard nitride coatings based on transition metals are widely used, such as CrAlN and TiAlN [2,3], CrMoN and CrTiN [4], ZrNbN [5], TiNbN [6], as well as superhard TiSiN and TiSiN/DLC hybrids [7] and TiN/DLC systems [8]. The classical monolayer nitrides – TiN, MoN, and NbN – which are characterized by high hardness (H ~ 20–30 GPa), low coefficient of friction, and good thermal and corrosion resistance – have been well studied and are widely used [9,10]. For TiN, it has been shown that structural refinement under the action of a substrate bias gradient increases the H/E and H^3/E^2 ratios and ensures high wear resistance [11]. For MoN-containing systems, a combination of increased hardness (up to ~28–30 GPa) and a low friction coefficient is achieved due to the formation of self-lubricating MoO_3 tribo-oxides [12] The NbN films demonstrate high hardness, wear resistance, and corrosion resistance simultaneously [13].

An analysis of modern scientific studies [12–15] in the field of structural materials and the development of the tooling industry indicates that for a long time the main attention has been focused on increasing the durability of protective coatings in order to extend the service life of components and tools. Thus, Chenrayan and co-authors showed that the application of TiAlN, DLC, and TiCN coatings to cutting tools provides an increase in tool life by approximately 5.8 times compared to uncoated tools [16]. In the work of Sonawane et al., it was demonstrated that, during dry turning of DSS2205 steel, a tool with an AlTiCrN coating achieves an operating time of about 124 minutes, which is roughly 3.5 times higher than that of an uncoated tool [17]. Akbar and co-authors established that the use of a multilayer TiAlN/TiN coating on carbide drills makes it possible to increase tool life by approximately six times compared with both uncoated and single-layer variants [18].

The evolution of coating deposition technologies has led to the development of advanced multifunctional and highly wear-resistant materials, thereby creating new opportunities for further optimization of their performance and expansion of their application domains. Xu et al. demonstrated that employing high-power impulse magnetron sputtering (HiPIMS) to fabricate multilayer MoN/TiN coatings results in a dense nanolamellar architecture with significantly enhanced mechanical and tribological properties compared with conventional deposition techniques, making these coatings promising candidates for heavily loaded tribological systems and cutting tools [12].

Zhang et al. developed a superhard high-entropy nitride coating, AlCrNbSiTiN, exhibiting an ultrahigh hardness of approximately 46 GPa and an exceptionally low wear rate of 6.3×10^{-7} $mm^3/N\cdot m$. Such outstanding performance suggests

Cite as: O.V. Maksakova, V.M. Beresnev, S.V. Lytovchenko, M. Čaplovičova, D.V. Horokh, B.O. Mazilin, M. Sahul, East Eur. J. Phys. 4, 701 (2025), https://doi.org/10.26565/2312-4334-2025-4-76

strong potential for applications in components operating under extreme mechanical stresses [19]. Furthermore, Wang and co-authors reported that AlCrNbSiTiN high-entropy nitride coatings deposited by RF magnetron sputtering combine high hardness with markedly improved corrosion resistance in water vapor environments, making them suitable for aggressive and high-temperature service conditions [20].

Recent findings [21] indicate that PEALD processing of Ti–Mo–N systems enables the formation of nitride coatings with excellent adhesion and very low wear, primarily due to precise control of the coating–substrate interface. Van Meter et al. established that the critical factor governing adhesion is the surface condition prior to deposition, specifically the presence of a native oxide layer on the substrate without any adhesion-promoting or buffer interlayers. This native-oxide interface minimized residual stresses in the TiMoN film and provided the strongest adhesion. Conversely, aggressive pre-deposition etch-cleaning increased compressive stresses and degraded interfacial strength. The optimal configuration is TiMoN deposited directly onto a native-oxidized substrate, which resulted in the lowest wear coefficient of ~4×10^{-8} $mm^3/N \cdot m$, underscoring the essential role of controlled interfacial engineering in achieving long-term durability of nitride coatings.

In a recent study, Zhou et al. [22] demonstrated that TiMoN coatings exhibit an atypical deformation behavior compared with conventional TMN hard-coating systems – plastic deformation occurs not through brittle fracture but via intensive dislocation multiplication and grain-boundary-mediated sliding. This dislocation-governed mechanism enables efficient dissipation of contact-induced energy and suppresses crack formation, which typically initiates abrasive or adhesive wear in traditional nitride coatings. Consequently, the intrinsic ability of TiMoN to undergo localized plastic deformation provides a basis for its enhanced wear resistance and improved stability under cyclic and impact loading conditions.

Further investigations of TiMoN-based systems confirm the promising potential of this composition. Zhou et al. reported that Mo-alloyed TiN coatings of the $TiMo_{0.08}N$ type, deposited by multi-arc ion plating, combine high hardness (up to ~34 GPa), strong adhesion (Lc > 65–100 N), and a low friction coefficient (< 0.24) due to the formation of a lubricious MoO_3 tribo-oxide in the wear track. These coatings also markedly reduced the corrosion current compared with WC–Co substrates [23]. Moreover, Wang et al. showed that TiMoN coatings deposited on GCr15 bearing steel by arc ion plating exhibit a minimum friction coefficient (≈ 0.31), a low wear rate of ~1.99×10^{-6} $mm^3/N \cdot m$, and a corrosion current of 3.62×10^{-9} A/cm^2 when an optimal substrate bias of −120 V is applied. These improvements were attributed to a pronounced (111) texture and the formation of a layered MoO_3 tribo-oxide phase, further confirming the potential of TiMoN systems as self-lubricating, wear-resistant coatings [24].

Although monolayer TiMoN coatings already exhibit atypical, dislocation-mediated plasticity and enhanced wear resistance compared with conventional TMN hard-coating systems, a logical next step is to transition to multilayer architectures. Direct examples of multilayer structures based on TiMoN remain limited and are mainly represented by the TiMoN/Si_3N4 system, in which the formation of a nanomultilayer configuration leads to increased hardness and reduced wear rates relative to monolithic TiMoN. These improvements arise from the periodic alternation of stiff and more compliant sublayers, as well as the high density of interlayer interfaces [25].

Comprehensive reviews on protective nanomultilayer nitride films indicate that such architectures typically provide higher hardness, improved oxidation stability, and lower wear rates than their corresponding single-layer nitrides. These advantages stem from interfacial dislocation blocking, crack deflection at layer boundaries, and the presence of a controlled stress gradient across the multilayer stack [26]. This behavior is further confirmed by specific examples such as TiN/NbN superlattices, where nanoscale layering periods simultaneously enhance adhesion, fracture resistance, and both corrosion and tribological stability [27].

On the other hand, NbN and multilayer systems incorporating NbN are increasingly regarded as a promising platform for wear-resistant coatings. NbN-based coatings exhibit elevated microhardness, a favorable state of compressive residual stress, and reduced temperature and stress at the cutting edge compared with TiN, which directly translates into extended tool life in machining applications. The transition to multilayer architectures with functional NbN-containing layers further enhances fracture resistance and overall tool performance. In particular, nanoscale WN/NbN coatings deposited by CA-PVD show high hardness values of ~33.6–36.6 GPa and low specific wear rates of $(1.9 – 4.1) \times 10^{-6}$ $mm^3/N \cdot m$, confirming the suitability of NbN as a rigid strengthening constituent in multilayer nitride systems [16].

Considering the low thermal conductivity of NbN and its ability to form protective oxide layers, combining TiMoN with NbN in a multilayer architecture can be expected to deliver a synergistic enhancement in wear resistance through several mechanisms. The hardness and elastic modulus contrast between TiMoN and NbN layers, which impedes crack propagation. The activation of dislocation-mediated plasticity in TiMoN layers, enabling efficient dissipation of contact energy. The formation of beneficial compressive residual stresses and a thermal-barrier effect provided by NbN sublayers. The potential development of “adaptive” tribo-oxides (MoO_3 and Nb_2O_5) that reduce the coefficient of friction. These combined effects position the TiMoN/NbN system as an up-and-coming candidate for the next generation of multilayer wear-resistant coatings.

Our previous investigations of TiMoN/NbN multilayer coatings demonstrated that the microstructure and mechanical response of the system are strongly governed by the combination of working pressure and applied substrate bias. It was established that deposition at −200 V and 0.52 Pa yields the highest layer density, well-defined interfaces, and

minimal microdefect content, which correlates with the maximum hardness of 31.6 GPa and an elastic modulus of 462 GPa. In contrast, deposition at 0.13 Pa results in blurred interfaces, reduced crystallinity, and an elevated density of microdefects, with microstrain nearly doubling from ~1.0×10^{-3} to ~2.1×10^{-3} [28]. These structural differences are expected to play a decisive role in the coating behavior under external loading, particularly in terms of wear resistance.

Given the established dependence of structural and mechanical properties of TiMoN/NbN coatings on nitrogen pressure during deposition, a key open question concerns how these differences manifest under actual sliding contact. It is well known that microstructure and interface quality govern wear behavior ranging from the formation of protective oxide films to localized plastic deformation or brittle fracture. Preliminary results indicate that the coating deposited at 0.52 Pa has a denser, more balanced architecture, whereas the 0.13 Pa coating exhibits greater defectiveness and Ti enrichment. However, the tribological response of these coatings, specifically their chemical evolution, the morphology of worn regions, and the role of possible tribo-oxides, has not yet been systematically examined.

Therefore, in this work, a comparative study was carried out to evaluate the wear resistance and wear mechanisms of TiMoN/NbN nano-multilayer coatings deposited at different nitrogen pressures (0.52 and 0.13 Pa), to identify the optimal deposition regime and gain deeper insight into the tribological processes governing the performance of such multilayer systems.

EXPERIMENTAL DETAILS

Deposition Process

The TiMoN/NbN multilayer coatings were deposited using cathodic-arc PVD, a technique distinguished by its high deposition rate and the substantial ion energies inherent to arc plasmas, which promote the formation of dense, well-adherent nitride layers even on substrates with complex geometries. The arc discharge generates multiply charged metal ions, creating favorable conditions for the growth of compact layers and for the strengthening of the near-surface region of the substrate.

For the experiments, 12X18H9T stainless steel plates with dimensions of 10 × 10 × 2.5 mm were used as substrates. The substrates were ground with 2000-grit abrasive paper and polished using a one micron diamond suspension. The Ti and Mo species were supplied from a sintered composite TiMo cathode with a Ti : Mo ratio of 80:20. At the same time, the NbN layers were deposited from a high-purity (99.8 %) niobium cathode. Nitrogen gas (N_2, 99.6 %) served as the reactive atmosphere. The substrates were ultrasonically cleaned in acetone, ethanol, and deionized water (25 min each) and then mounted on a vertical sample holder inside the chamber. The base pressure was reduced to ~4×10^{-3} Pa to minimize oxygen contamination.

The coatings were deposited for 90 minutes at various working nitrogen pressures (0.13 and 0.52 Pa) and negative substrate bias of –200 V. The cathode currents were set to 110 A for the TiMo target and 90 A for Nb target. The multilayer architecture was achieved by continuous rotation of the substrate holder, ensuring uniform layer growth. The deposition regimes are summarized in Table 1.

Table 1. Deposition parameters of the TiMoN/NbN nano-multilayer coatings

Sample	Arc current, A	Substrate bias, V	N2 pressure, Pa	Deposition time, min
1552(TiMoN/NbN)	110/90	-200	0.52	90
1554(TiMoN/NbN)			0.13	

Characterization

The cross-sectional microstructure at multiple magnifications and the morphology of the worn surfaces were characterized using field-emission scanning electron microscopy (FE-SEM) employing Quanta 600 FEG and FEI Nova NanoSEM 450 microscopes operated at accelerating voltage of 20 kV. The acquired images were used to assess the columnar growth characteristics and to determine the thickness and uniformity of the individual nanolayers. In addition, the wear tracks were examined to evaluate their microstructure and elemental composition.

Ball-on-disc tribological tests were conducted using a Bruker UMT-2 universal tribometer. A 6.3 mm WC–Co ball was employed as the counterbody. The tests were performed under a normal load of 5 N at a rotational speed of 200 rpm for a total sliding duration of 30 min. The sliding radius was maintained constant throughout the experiment, and the corresponding linear sliding speed was adjusted accordingly. The tests were carried out under ambient laboratory conditions (22–24 °C, relative humidity 35–45 %), and no lubrication was applied. The evolution of friction during sliding was continuously recorded to obtain the friction coefficient as a function of time.

RESULTS AND DISCUSSIONS

The TiMoN/NbN nano-multilayer coatings deposited at different working nitrogen pressures (0.52 and 0.13 Pa) will exhibit fundamentally distinct tribological behaviors directly governed by the structural integrity of the nanolayers, the quality of the interfaces, and the chemistry of the tribofilm formed during sliding. Despite having comparable total thicknesses (~10–11 μm) and similar numbers of periods (~270), the sequence of alternating hard NbN and more compliant TiMoN layers and, critically, the defect density at their interfaces determines the mechanical response of the system under cyclic contact loading.

The cross-sectional SEM images of TiMoN/NbN nano-multilayer coatings are shown in Fig. 1. It is evident that both coatings exhibit a well-defined, nearly perfectly parallel multilayer architecture in which the NbN layers act as structural "reinforcement ribs." These layers uniformly distribute the applied load and serve as effective barriers to dislocation propagation.

The cross-sectional SEM images of TiMoN/NbN nano-multilayer coatings are shown in Fig. 1. It is evident that both coatings exhibit a well-defined, nearly perfectly parallel multilayer architecture in which the NbN layers act as structural "reinforcement ribs." These layers are supposed to uniformly distribute the applied load and serve as effective barriers to dislocation propagation. Although both coatings exhibit a clearly developed multilayer architecture, the cross-sectional images reveal subtle but technologically significant differences in the microstructural quality as a function of the nitrogen pressure. The coating deposited at 0.52 Pa (sample 1552) shows a highly compact, slightly columnar morphology with straight, well-defined, and sharply delineated interfaces between adjacent nanolayers. The individual TiMoN/NbN periods maintain a nearly constant thickness across the entire coating cross section, and the interlayer boundaries appear clean and continuous, indicating a stable growth regime with suppressed defect formation. In contrast, the coating grown at 0.13 Pa (sample 1554) also forms a multilayer stack, yet the nanolayers do not exhibit a columnar structure. However, it is evident that there is a higher density of microdroplet-related defects, which is typical of low-pressure arc evaporation. While the periodicity is preserved, the interfaces in sample 1554 appear locally less sharp and occasionally broadened, suggesting less effective kinetic energy dissipation during layer formation and reduced adatom mobility. These microstructural distinctions, namely, the higher layer density, cleaner interfaces, and reduced defect concentration in sample 1552, play a decisive role in its superior mechanical response under sliding contact and correlate directly with the stability of the friction coefficient and the robustness of the tribofilm formed during wear.

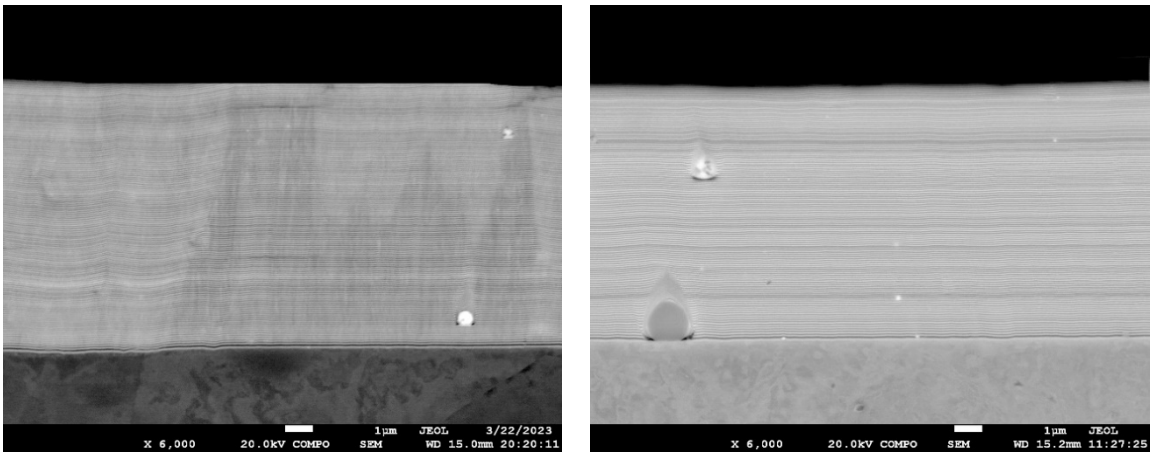

a b

Figure 1. Cross-sectional SEM images of TiMoN/NbN nano-multilayer coatings deposited at different working nitrogen pressures: (a) 0.52 Pa and (b) 0.13 Pa

A comparative analysis of the elemental composition of the as-deposited TiMoN/NbN nano-multilayer coatings (Table 2) reveals pronounced differences that arise already at the deposition stage under different nitrogen pressures. Sample 1552 contains a higher fraction of titanium (36.71 wt. %) and a slightly lower fraction of niobium (42.48 wt. %) compared with sample 1554, which suggests a more uniform growth of the TiMoN sublayers and a better-stabilized superlattice structure at the higher reactive-gas pressure. In contrast, sample 1554 exhibits substantial niobium enrichment (46.92 wt. %) accompanied by a reduction in titanium content to 14.94 wt. %, indicating a change in the layer growth mechanism and a possible dominance of NbN in the nanolayers under low-pressure conditions. The moderately increased molybdenum content in 1554 is also consistent with deposition conditions that promote a local redistribution of metallic constituents toward Nb–Mo enrichment. Such compositional variations directly influence the microstructure, residual stress state, and, ultimately, the tribological performance of the coatings.

Table 2. Elemental composition of the TiMoN/NbN nano-multilayer coatings deposited at different working nitrogen pressures: (a) 0.52 Pa and (b) 0.13 Pa.

Element	1552(TiMoN/NbN)		1554(TiMoN/NbN)	
	wt. %	at. %	wt. %	at. %
N	18.02	48.30	14.94	37.57
Ti	36.71	30.20	32.98	30.45
Nb	42.48	18.02	46.92	24.23
Mo	2.79	3.48	5.16	7.75
Total	100.00	100.00	100.00	100.00

The friction–time curves shown in Fig. 2 demonstrate that sample 1552 maintains a stable sliding response with a COF of approximately 0.42–0.48 throughout nearly the entire test. The initial running-in stage (COF increasing from ~0.20 to

~0.45 within the first 10–20 s) gradually transitions into a regime dominated by the formation of a self-sustaining oxide–nitride tribofilm, which effectively suppresses stress fluctuations and prevents a shift toward abrasive wear.

In contrast, the COF of sample 1554 progressively rises to 0.60–0.70 and exhibits periodic spikes corresponding to repeated cycles of tribofilm breakdown and localized reformation. This behavior indicates the predominance of abrasive–adhesive wear mechanisms and the absence of a stable lubricious phase at the sliding interface.

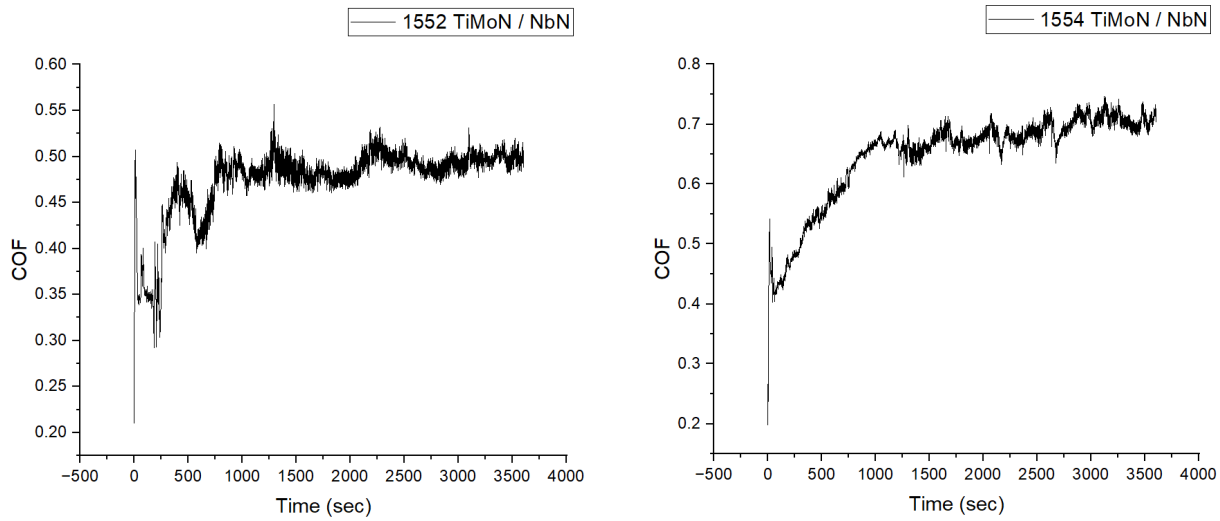

a b

Figure 2. Evolution of the friction coefficient of the TiMoN/NbN nano-multilayer coatings deposited at different working nitrogen pressures: (a) 0.52 Pa and (b) 0.13 Pa.

The morphology of the wear tracks of the TiMoN/NbN nano-multilayer coatings deposited at different working nitrogen pressures is presented in Fig. 3. The results shows a striking contrast between the two deposition regimes. The wear track of sample 1552 exhibits smooth, well-aligned sliding marks with only faint groove formation, indicative of a weak abrasive component in the overall wear process. By contrast, sample 1554 shows deeper grooves, numerous micro-pullouts, and distinct regions of transferred counterbody material (W–Co), confirming a combined abrasive–adhesive wear mechanism. This mode of degradation points to the absence of a stable protective tribofilm and to local coating failure extending down to the sublayer level.

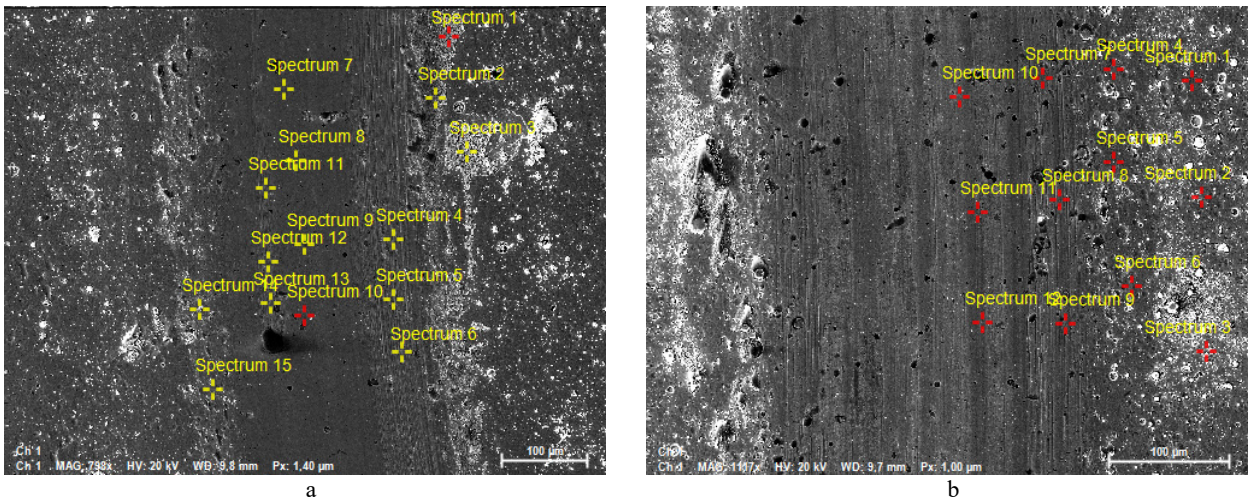

a b

Figure 3. Wear tracks on the surface of the TiMoN/NbN nano-multilayer coatings deposited at different working nitrogen pressures: (a) 0.52 Pa and (b) 0.13 Pa.

The TiMoN layers likely exhibit the dislocation-mediated plasticity characteristic of TiMoN-based systems: intensive dislocation multiplication and grain-boundary sliding enable localized dissipation of frictional energy without the formation of brittle cracks. As a result, the multilayer structure attains an adaptive load-bearing response in which the "rigid" NbN and more "compliant" TiMoN sublayers operate synergistically.

The EDS analysis of the worn surface regions enables a direct correlation between the chemical nature of the tribofilm and the distinct tribological responses of the coatings. Table 3 presents the elemental composition of the wear track obtained at different regions of the sample 1552. Across the width of the wear track, the elemental distribution in sample 1552 exhibits behavior characteristic of stable adaptive tribosystems. The periphery is covered with thick,

predominantly titanium-rich oxides (O = 70–75 wt. %, Ti < 25 wt. %), which play minimal functional roles during sliding. In contrast, the central region develops a thin, compact, and mechanically robust tribofilm with a balanced Ti−Nb−Mo−O composition (O = 13–19 wt %, Ti = 38–42 wt. %, Nb = 37–40 wt. %, Mo = 5–6 wt. %). The elevated fractions of Mo and Nb in the central zone point to the formation of lubricious MoO_3 and strengthening Nb_2O_5 phases, while Ti probably contributes through the formation of stable TiO_2 oxides. This multicomponent adaptive tribofilm is responsible for the low friction coefficient and smooth sliding behavior of sample 1552.

Table 3. Elemental composition of the wear track of the TiMoN/NbN nano-multilayer coating (1552) in wt. %.

Spectrum No	O	Ti	Fe	Nb	Mo	W
Sp. 1	71.99	13.20	0.92	11.29	2.33	0.02
Sp. 2	75.35	11.47	1.04	10.08	1.81	0.01
Sp. 3	46.16	23.93	0.50	24.77	4.00	0.29
Sp. 4	13.37	41.48	0.06	38.55	5.80	0.04
Sp. 5	15.51	40.00	0.04	37.79	5.92	-
Sp. 6	14.19	40.58	0.00	38.64	6.07	-
Sp. 7	16.28	39.96	0.20	37.29	5.63	-
Sp. 8	18.35	39.61	0.13	35.70	5.60	0.07
Sp. 9	13.75	41.00	0.14	38.23	6.09	-
Sp. 10	12.38	41.38	0.05	39.40	6.05	-
Sp. 11	15.21	39.90	0.14	38.28	5.77	0.05
Sp. 12	29.53	32.85	0.20	31.30	5.63	-
Sp. 13	31.65	32.06	0.04	31.04	4.65	-
Sp. 14	69.39	14.02	0.42	13.58	2.33	0.04
Sp. 15	30.44	33.96	0.04	30.16	4.97	-

The elemental composition of the wear track obtained at different regions of the sample 1554 is presented in Table 4. It indicates the absence of a well-developed adaptive tribofilm, in sharp contrast to the behavior observed for sample 1552. Across the entire width of the wear track, the oxygen content remains low (O = 8–14 wt. %), suggesting the formation of only a thin and brittle TiO_2 layer rather than complex Ti–Mo–Nb–O oxides. The high titanium content (Ti = 46–55 wt. %) together with the relatively uniform distribution of niobium (Nb = 27–32 wt. %) implies exposure and progressive degradation of the outer TiMoN layers rather than the formation of the strengthening Nb_2O_5 phase typically associated with stable tribosystems.

Although molybdenum is present at a measurable level (5–6 wt %), the limited degree of oxidation prevents the development of lubricious MoO_3, depriving the coating of an intrinsic friction-reducing mechanism. Consequently, the tribofilm formed on sample 1554 is thin, heterogeneous, and brittle, lacking any self-replenishing capability. This unstable surface layer readily breaks down under load, resulting in a dominant abrasive–adhesive wear mechanism and a correspondingly elevated friction coefficient.

Table 4. Elemental composition of the wear track of the TiMoN/NbN nano-multilayer coating (1554) in wt. %.

Spectrum No	O	Ti	Fe	Nb	Mo	W
Sp. 1	8.17	54.34	0.08	30.50	6.21	-
Sp. 2	11.74	53.47	0.10	27.93	6.11	-
Sp. 3	23.11	46.04	0.05	25.19	5.09	-
Sp. 4	8.48	54.03	-	30.70	6.09	-
Sp. 5	23.71	47.25	-	14.29	13.86	0.01
Sp. 6	12.27	53.04	-	28.39	5.83	-
Sp. 7	5.88	55.03	-	32.11	6.16	0.09
Sp. 8	9.54	54.25	0.10	29.58	5.96	0.02
Sp. 9	9.88	52.97	-	30.43	6.14	-
Sp. 10	9.16	55.06	-	29.30	5.86	-
Sp. 11	13.68	51.93	-	27.94	5.82	0.09
Sp. 12	12.71	52.89	0.04	28.23	5.53	-

Overall, the obtained results clearly demonstrate that the wear resistance of the TiMoN/NbN nano-multilayer coatings is governed not only by the presence of NbN sublayers but, critically, by the degree to which they are structurally integrated into the multilayer architecture. The higher at working nitrogen pressure (0.52 Pa) promotes uniform layer alternation, which facilitates the formation of a stable adaptive tribofilm and enables efficient dissipation of mechanical energy through controlled TiMoN-mediated plasticity. Under lower working nitrogen pressure (0.13 Pa), however, the increased defect density and disrupted periodicity of the nanolayers diminish the stabilizing role of NbN, yielding a tribofilm that is thin, brittle, and spatially heterogeneous.

These microstructural distinctions ultimately dictate whether the TiMoN with NbN layers' sequence operates as an effective nanolaminate capable of crack deflection, adaptive load partitioning, and generating lubricious MoO_3 phases or transitions into an unstable sliding regime dominated by abrasive and adhesive wear processes.

CONCLUSIONS

This work provides a comprehensive assessment of the wear behaviour of TiMoN/NbN nano-multilayer coatings deposited by CA-PVD at two markedly different working nitrogen pressures (0.52 and 0.13 Pa). The combined structural, chemical, and tribological analyses clearly demonstrate that the wear performance of these multilayer systems is governed not simply by their nominal composition or the presence of alternating TiMoN and NbN layers, but critically by the degree of structural order, interface integrity, and the capacity of the coating to generate a functional tribofilm during sliding contact.

Deposition at the higher nitrogen pressure (0.52 Pa) results in a well-organized multilayer architecture with sharply defined and nearly perfectly parallel interfaces. This structural coherence minimizes microstrain, suppresses defect formation, and ensures a more homogeneous distribution of Ti, Nb, and Mo throughout the multilayer stack. Under sliding conditions, these features enable the formation of a robust, multicomponent adaptive tribofilm enriched in TiO_2, Nb_2O_5, and MoO_3 phases. The presence of MoO_3 contributes lubricious properties, while Nb_2O_5 enhances thermal and mechanical stability. As a result, the coating demonstrates a consistently low friction coefficient and limited wear, confirming the synergistic action of stiff NbN layers and plastically accommodating TiMoN layers.

In contrast, deposition under low nitrogen pressure (0.13 Pa) leads to significant structural degradation. The altered metal distribution – particularly the reduced titanium content in the as-deposited state and the inability to generate oxidized Mo- or Nb-rich phases during wear – prevents the formation of a stabilizing tribofilm. Instead, only a thin, brittle TiO_2 film develops, which lacks both mechanical robustness and self-replenishing characteristics. Consequently, the coating is prone to abrasive–adhesive wear, exhibits substantial counterbody transfer, and manifests a high, unstable friction coefficient.

The comparative analysis unequivocally shows that the tribological response of TiMoN/NbN nano-multilayer systems depends on the interplay between: (i) structural periodicity and interface sharpness; (ii) microdefect density and residual stress distribution; and (iii) the chemistry and adaptability of tribofilm formation. Coatings deposited at 0.52 Pa satisfy all three requirements, yielding an optimized nanolaminate capable of crack deflection, controlled energy dissipation through TiMoN-mediated plasticity, and formation of a lubricious, strengthening tribofilm. Those deposited at 0.13 Pa fail to meet these criteria, leading to unstable friction and accelerated wear.

Overall, the study demonstrates that precise control of working nitrogen pressure during CA-PVD deposition is a determining factor for tailoring the structural integrity and tribological performance of TiMoN/NbN nano-multilayer coatings. The findings highlight the strong potential of these materials for advanced wear-critical applications, provided that deposition conditions are optimized to promote coherent multilayer architectures and the formation of effective adaptive tribofilms.

Acknowledgments

Funded by the EU NextGenerationEU through the Recovery and Resilience Plan for Slovakia under project No. 09I03-03-V01-00028. The Ukrainian state budget program under project No. 0124U001127 also supports this research.

ORCID

Olga Maksakova, https://orcid.org/0000-0002-0646-6704; **Vyacheslav Beresnev**, https://orcid.org/0000-0002-4623-3243;
Serhiy Lytovchenko, https://orcid.org/0000-0002-3292-5468; **Mária Čaplovičová**, https://orcid.org/0000-0003-4767-8823;
D.V. Horokh, https://orcid.org/0000-0002-6222-4574; **B.O. Mazilin,** https://orcid.org/0000-0003-1576-0590;
M. Sahul, https://orcid.org/0000-0001-9472-500X

REFERENCES

[1] W. Li, P. Liu, and P.K. Liaw, Mater. Res. Lett. **6**(4), 199 (2018). https://doi.org/10.1080/21663831.2018.1434248
[2] R. Lin, S. Sun, B. You, T. Dong, Y. Sui, and S. Wei, Mater. Res. Express. **11**, 096402 (2024). https://doi.org/10.1088/2053-1591/ad7350
[3] J. Liu, Y. Wang, G. Liu, J. Hua, and X. Deng, Coatings, **13**(7), 1229 (2023), https://doi.org/10.3390/coatings13071229
[4] K. S. Surendra Mohan, S. Gunasekaran, D. Manjubashini, S. Umayal, S. Sivaranjani, and B. Subramanian, J. of Materi Eng and Perform **33**, 10614–10622 (2024). https://doi.org/10.1007/s11665-023-08691-x
[5] S. Zhang, N. Wang, D.J. Li, L. Dong, H.Q. Gu, R.X. Wan, and X. Sun, Nuclear Instruments and Methods in Physics Research Section B: Beam Interactions with Materials and Atoms, **307**, 119-122 (2013). https://doi.org/10.1016/j.nimb.2012.12.067.
[6] H. Dempwolf, M. Proft, A. Baumann, S. Malz, O. Keßler, Coatings, **12**, 935 (2022). https://doi.org/10.3390/coatings12070935
[7] N. Vattanaprateep, N. Panich, and P. Surin, Journal of Southwest Jiaotong University, **58**(6), (2023). https://doi.org/10.35741/issn.0258-2724.58.6.25
[8] Z. Xia, W. Song, H. Yu, X. Li, Y. Yin, and W. Xie, Coatings, **15**(10), 1150 (2025). https://doi.org/10.3390/coatings15101150
[9] J. Chen, S. Zhang, J. Li, Z. Chen, and D. Sun, Surface and Coatings Technology, **497,** 131800 (2025). https://doi.org/10.1016/j.surfcoat.2025.131800
[10] Y. Wang, W. Yuan, W. Han, J. Gao, H. Li, and T. Zhao, Ceramics International, **50**(6), 9460-9468 (2024). https://doi.org/10.1016/j.ceramint.2023.12.263
[11] Y.H. Wang, F. Guo, H. Ren, S.Y. Hu, Y.J. Chen, Y.H. Zhao, F. Gong, and Z.W. Xie, Ceramics International, **48**(6), 8746–8750 (2022). https://doi.org/10.1016/j.ceramint.2022.01.010
[12] J. Xu, P. Zhang, J. Yu, P. Ying, T. Yang, J. Wu, T. Wang, N. Myshkin, and V. Levchenko, Lubricants, **13**(8), 319 (2025). https://doi.org/10.3390/lubricants13080319

[13] Q. Guo, K. Wang, T. Fang, D. Zhang, H. Sun, and Y. Wan, Advanced Engineering Materials, **27**(18), 2500974 (2025). https://doi.org/10.1002/adem.202500974
[14] B. Warcholinski, A. Gilewicz, K. Kminikowska, A.S. Kuprin, G.N. Tolmachova, E.N. Reshetnyak, I.V. Kolodiy, *et, al.,* Wear, **578-579,** 206224 (2025). https://doi.org/10.1016/j.wear.2025.206224
[15] K. Smyrnova, M. Sahul, M. Haršáni, V. Beresnev, M. Truchlý, L. Čaplovič, M. Čaplovičová, *et al.,* ACS Omega, **9** (15), 17247-17265 (2024). https://doi.org/10.1021/acsomega.3c10242
[16] V. Chenrayan, C. Manivannan, K. Shahapurkar, A. Krishna, V. Tirth, A. Algahtani, and I.M. Alarifi, *et al.,* Journal of Nanomaterials, **2022**(1), 9664365 (2022). https://doi.org/10.1155/2022/9664365
[17] G.D. Sonawane, R. Bachhav, and A. Barnwal, JOM, **76**, 313–326 (2024). https://doi.org/10.1007/s11837-023-05991-4
[18] F. Akbar, and M. Arsalan, Proceedings of the Institution of Mechanical Engineers, Part B: Journal of Engineering Manufacture, **238**(1-2), 95-107 (2023). https://doi.org/10.1177/09544054231157247
[19] X. Zhang, Z. Zeng, X. Zeng, V. Pelenovich, Q. Wan, A. Pogrebnjak, L. Xue, *et al.,* Materials Research Letters, **13**(2), 103–112 (2024). https://doi.org/10.1080/21663831.2024.2425167
[20] X. Wang, J. Liu, Y. Liu, W. Li, Y. Chen, and B. Yang, Coatings, **14**(8), 1006 (2024). https://doi.org/10.3390/coatings14081006
[21] K. Van Meter, Md.I. Chowdhury, T. Babuska, Jewel Haik, T. Tanasarnsopaporn, M.J. Sowa, A.C. Kozen, *et al.,* Wear, **570**, 205980 (2025). https://doi.org/10.1016/j.wear.2025.205980
[22] S. Zhou, Z. Qiu, Z. Wang, W. Yang, and A. Wang, Rare Metals, **44**(5), 2845-2852 (2025). https://doi.org/10.1007/s12598-024-03128-3
[23] S. Zhou, W. Zhao, Y. Wu, Z. Qiu, S. Lin, Z. Zheng, and D.C. Zeng, Vacuum, **190**, 110311 (2021). https://doi.org/10.1016/j.vacuum.2021.110311
[24] C. Wang, J. Liu, G. Liu, L. Xue, and K. Zhang, Coatings, **15**(8):956 (2025). https://doi.org/10.3390/coatings15080956
[25] T. Wang, G. Zhang, and B. Jiang, Applied Surface Science, **326**, 162-167 (2015). https://doi.org/10.1016/j.apsusc.2014.11.125
[26] W. Cheng, J. Wang, X. Ma, P. Liu, P.K. Liaw, and W. Li, Journal of Materials Research and Technology, **27,** 2413-2442 (2023). https://doi.org/10.1016/j.jmrt.2023.10.012
[27] AA. Sugumaran, Y. Purandare K. Shukla,I. Khan, A. Ehiasarian, and P. Hovsepian, Coatings, **11**, 867 (2021). https://doi.org/10.3390/coatings11070867
[28] O. Maksakova, V. Beresnev, M. Caplovicova, Z. Zhang, M. Sahul, S. Lytovchenko, and B. Mazilin, in: *IEEE 15th International Conference Nanomaterials: Applications & Properties (NAP)* (Bratislava, Slovakia, 2025), pp. MTFC03-1-MTFC03-5. https://doi.org/10.1109/NAP68437.2025.11216249

ДОСЛІДЖЕННЯ ЗНОСОСТІЙКОСТІ TiMoN/NbN НАНОБАГАТОШАРОВИХ ПОКРИТТІВ, ОСАДЖЕНИХ ВАКУУМНО-ДУГОВОЮ ТЕХНОЛОГІЄЮ ЗА РІЗНИХ РОБОЧИХ ТИСКІВ

О.В. Максакова[1,2], В.М. Береснєв[2], С.В. Литовченко[2], М. Чапловичова[3], Д.В. Горох[2], Б.О. Мазілін[2], М. Сахул[1]
[1]Інститут матеріалознавства, Словацький технологічний університет у Братиславі, вул. Яна Ботту 25, 917 24, Трнава, Словаччина
[2]Харківський національний університет імені В.Н. Каразіна, майд. Свободи, 4, 61000, Харків, Україна
[3]Центр нанодіагностики матеріалів, Словацький технологічний університет у Братиславі, Вазовова 5, 812 43, Братислава, Словаччина

Дане дослідження присвячене аналізу зносостійкості нанобагатошарових покриттів TiMoN/NbN, осаджених методом катодно-дугового PVD за різних робочих тисків азоту (0.52 та 0.13 Па). Хоча обидва покриття мають подібну загальну товщину (~10-11 мкм) і близьку кількість періодів (~270), їх структурна цілісність, якість інтерфейсів та елементний розподіл суттєво відрізняються залежно від тиску під час осадження. Покриття, синтезоване при 0.52 Па, формує високовпорядковану та щільну багатошарову архітектуру з чітко визначеними межами та зниженою концентрацією мікродефектів. Натомість покриття, отримане при 0.13 Па, характеризується вираженою хвилястістю меж, порушенням періодичності та зростанням дефектності. Трибологічні випробування «кулька–диск» показали стабільний коефіцієнт тертя 0.42–0.48 для покриття, отриманого при 0.52 Па, тоді як покриття, синтезоване при 0.13 Па, демонструє підвищений і нестабільний коефіцієнт тертя (0.60–0.70) з частими коливаннями. Мікроструктурний та хімічний аналізи доріжок зношування вказують на формування у покритті, отриманому при високому тиску, міцної адаптивної Ti–Nb–Mo–O трибоплівки, яка містить мастильні фази MoO_3 і зміцнювальні фази Nb_2O_5. У випадку низького тиску на поверхні формується лише тонка, крихка TiO_2-вмісна плівка, що не має здатності до самовідновлення. Отримані результати демонструють, що оптимізація тиску азоту є ключовою умовою для формування структурно узгоджених наноламінатів, здатних утворювати функціональні трибоплівки, що суттєво підвищує зносостійкість нанобагатошарових систем TiMoN/NbN.

Ключові слова: *вакуумно-дугова технологія; нітриди; багатошарові покриття; мікроструктура; склад; зносостійкість*